

RADC-TR-78-76
Interim Technical Report
March 1978

Scientific Report No. 31

EXCITATION OF CURRENT ON AN INFINITE HORIZONTAL WIRE
OVER THE EARTH BY AN ARBITRARY ELECTRIC DIPOLE SOURCE

by

Ahmed Hoorfar, Edward F. Kuester and David C. Chang

March 1978

Department of Electrical Engineering
University of Colorado

Approved for public release; distribution unlimited

ROME AIR DEVELOPMENT CENTER
AIR FORCE SYSTEMS COMMAND
GRIFFIS AIR FORCE BASE, NEW YORK 13441

UNCLASSIFIED

SECURITY CLASSIFICATION OF THIS PAGE (When Data Entered)

REPORT DOCUMENTATION PAGE		READ INSTRUCTIONS BEFORE COMPLETING FORM
1. REPORT NUMBER RADC-TR-78-76	2. GOVT ACCESSION NO.	3. RECIPIENT'S CATALOG NUMBER
4. TITLE (and Subtitle) EXCITATION OF CURRENT ON AN INFINITE HORIZONTAL WIRE OVER THE EARTH BY AN ARBITRARY ELECTRIC DIPOLE SOURCE		5. TYPE OF REPORT & PERIOD COVERED Scientific Report
		6. PERFORMING ORG. REPORT NUMBER Scientific Report No. 5
7. AUTHOR(s) Ahmed Hoorfar Edward F. Kuester David C. Chang		8. CONTRACT OR GRANT NUMBER(s) F19628-77-C-0093
9. PERFORMING ORGANIZATION NAME AND ADDRESS Electromagnetics Laboratory, Dept. of Elec. Engr. University of Colorado Boulder CO 80309		10. PROGRAM ELEMENT, PROJECT, TASK AREA & WORK UNIT NUMBERS 61102F 2305J321
11. CONTROLLING OFFICE NAME AND ADDRESS Deputy for Electronic Technology (RADC) Hanscom AFB MA 01731 Monitor/John Antonucci/EEC		12. REPORT DATE March 1978
		13. NUMBER OF PAGES
14. MONITORING AGENCY NAME & ADDRESS (if different from Controlling Office)		15. SECURITY CLASS. (of this report) UNCLASSIFIED
		15a. DECLASSIFICATION/DOWNGRADING SCHEDULE N/A
16. DISTRIBUTION STATEMENT (of this Report) Approved for public release; distribution unlimited.		
17. DISTRIBUTION STATEMENT (of the abstract entered in Block 20, if different from Report)		
18. SUPPLEMENTARY NOTES RADC Project Engineer: J. D. Antonucci (ETEP)		
19. KEY WORDS (Continue on reverse side if necessary and identify by block number) dipole excitation wire above earth scattering due to dielectric obstacles earth-attached modes transmission-line mode		
20. ABSTRACT (Continue on reverse side if necessary and identify by block number) Excitation of propagating modes on a long horizontal wire over the earth by an arbitrary oriented dipole source is investigated. It is shown that with proper tailoring of sources, it is feasible to provide stronger excitation for either the structured-attached mode or the earth-attached mode relative to the others. In general, because the transmission-line (structured-attached) mode usually has higher attenuation in the frequency range of interest, larger percentage change in total current due to the scattering obstacles can be achieved (Cont'd)		

UNCLASSIFIED

SECURITY CLASSIFICATION OF THIS PAGE(When Data Entered)

Item 20 (Cont'd)

when a smaller wire height is used. Numerical result for scattering due to dielectric obstacles modeling human bodies is included.

UNCLASSIFIED

SECURITY CLASSIFICATION OF THIS PAGE(When Data Entered)

TABLE OF CONTENTS

<u>Section</u>	<u>Page</u>
1. Introduction	1
2. Excitation by a Dipole Source: Formulation.	3
3. Current induced on the wire by a VED	10
4. Scattering by an ellipsoidal dielectric obstacle	20
5. Conclusion	29
Appendix A	31
References	35

EXCITATION OF CURRENT ON AN INFINITE HORIZONTAL WIRE
OVER THE EARTH BY AN ARBITRARY ELECTRIC DIPOLE SOURCE

by

Ahmed Hoorfar, Edward F. Kuester and David C. Chang

1. Introduction

The propagation of discrete modes along an infinite, thin, horizontal wire located above the surface of the earth has been studied by many authors ([1-3]; see also the bibliography in [4]). Until recently, however, no attempt had been made to study the excitation of these modes by anything other than a delta-function generator in the wire. Kuester and Chang [4] have given formulas for the excitation coefficients for an arbitrary distribution of external current sources, while Wait [5] discussed the special case of a vertical electric dipole (VED) source, and also the quasi-static limit. Olsen and Usta [6] also discuss this special case, and study the limiting case of large distances away from the dipole along the wire. The somewhat simpler situation of a perfectly conducting earth is investigated in [7]. Virtually no numerical results are available for the actual current induced on the wire as a function of dipole position. In fact, even for the much simpler case of a dipole exciting a wire in free space, only some analytical approximations for the current at large distances from the dipole seem to be available [8,9].

The dipole excitation problem is of interest for a number of practical applications. One is the problem of interference on open wire communications from external radiators. Another might be the distortion caused by a long wire such as a power line on the fields of a small transmitter used in a

used in a direction-finding scheme. The immediate motivation for the present investigation, however, is the problem of mode conversion caused by the proximity of a scattering object to a line propagating a discrete mode. It is possible that such a mechanism might be useful in an intruder detection system employing a long cable located in, on, or above the ground at the periphery of the region to be guarded. An intruder disturbing the fields of the mode normally propagating along the wire would cause a change in response at a monitoring station at the end of the wire. A number of potential instrumentation schemes have been proposed [10-12].

In the first part of this report, based upon the formulation given in [4], an expression for the current induced on a horizontal wire above the ground by an arbitrarily-oriented Hertzian electric dipole is presented. The total current is the sum of discrete modal contributions as well as a number of branch cut integrals corresponding to radiation spectra. These currents are evaluated numerically for a variety of dipole orientations, and locations with respect to the wire. It is found that certain configurations can excite the recently discovered earth-attached mode [13] with significant amplitude compared to either the ordinary transmission-line (or structure-attached) mode, or the radiation modes.

In the second part, the scattering of a mode incident onto a dielectric obstacle in proximity to the wire is studied. By using a Rayleigh approximation [14] for the induced polarization currents in the obstacle, its effect can be replaced by that of an electric dipole of appropriate intensity and orientation. The conversion of current into other modes (discrete as well as radiation modes) is examined, and the feasibility of this mechanism for the detection of human or animal intruders is discussed.

2. Excitation by a Dipole Source: Formulation

The configuration to be analyzed is depicted in Fig. 1. An arbitrarily oriented electric Hertzian dipole is located in the air at a point $P(x_0, y_0, z_0)$ as shown ($x_0 > 0$), above a conducting earth ($x < 0$) with electrical parameters ϵ , μ and σ . The dipole excites an infinite horizontal wire of radius a located at a height $x = h$ above the earth's surface, and at $y = 0$. The earth is assumed to be homogeneous, and a complex refractive index n is defined for it as

$$n = \left(\epsilon_r + \frac{i\sigma}{\omega\epsilon_0} \right)^{\frac{1}{2}}$$

with $\text{Im}(n) \geq 0$, appropriate to an $\exp(-i\omega t)$ time dependence, which will be suppressed hereafter. It is further assumed that $a \ll h$ and $k_0 a \ll 1$, so that the thin wire approximation, which postulates a uniform current distribution about the circumference of the wire surface, can be invoked.

The integral equation for the total current induced on the wire by a vertical electric dipole source has been derived by Wait [5] and by Olsen and Usta [6]. A more general formulation valid for an arbitrary source configuration is given by Kuester and Chang [4]. According to their results, the induced current on the wire is given as a Fourier integral

$$I(z) = \int_{-\infty}^{\infty} \tilde{I}(\alpha) e^{ik_0 \alpha z} d\alpha \quad (1)$$

where $k_0 = \omega\sqrt{\mu_0\epsilon_0}$ is the wavenumber in air. Using a reciprocity argument, the transform function $\tilde{I}(\alpha)$ is obtained as an integration of the product of the source current distribution with the fields produced by a current on the wire. If only external electric currents are present,

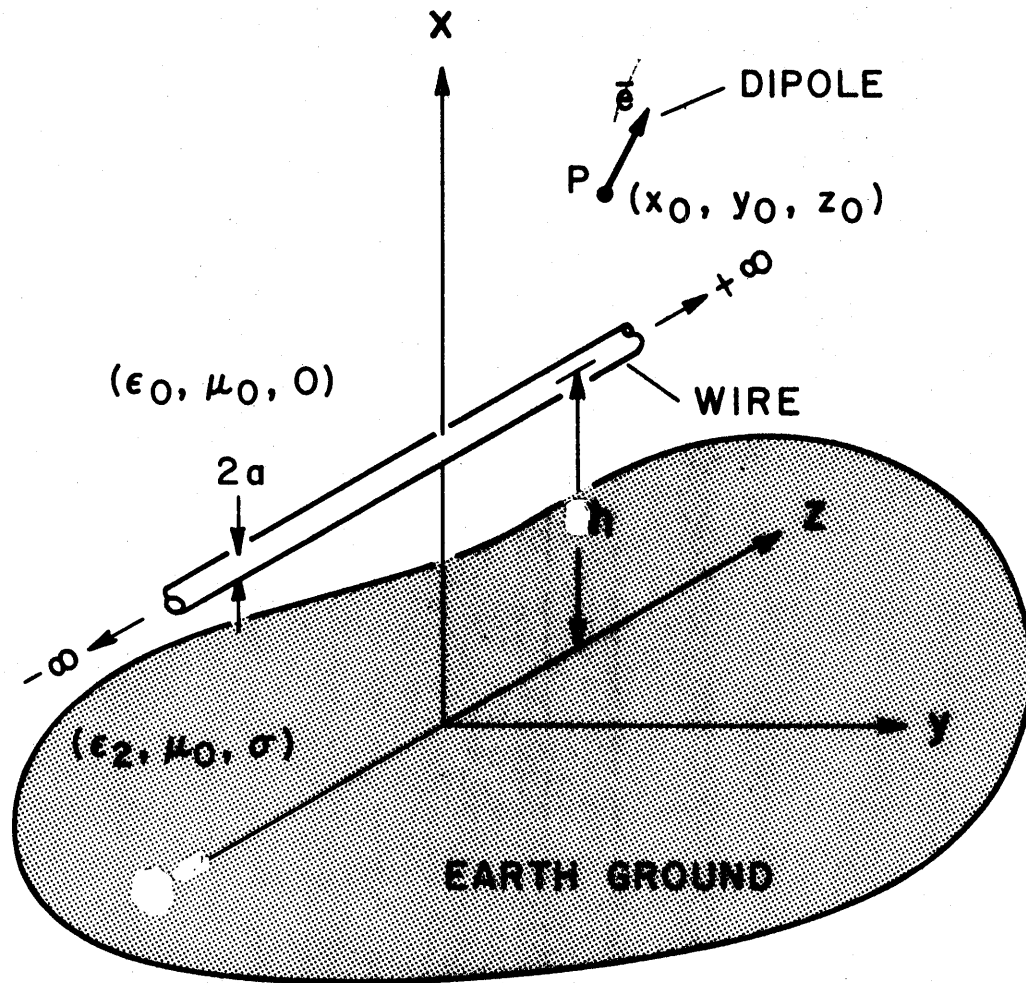


Figure 1. Geometry of the problem

$$\tilde{I}(\alpha) = \frac{4}{\eta_0 k_0 \tilde{M}(\alpha)} \iiint_V \tilde{\mathbf{E}}_0^w(\bar{\mathbf{x}}_t; -\alpha) \cdot \bar{\mathbf{J}}_e^{\text{ext}}(\bar{\mathbf{x}}) e^{-ik_0 \alpha z} dV \quad (2)$$

In (2), $\tilde{\mathbf{E}}_0^w$ is given more specifically by

$$\tilde{\mathbf{E}}_0^w(\bar{\mathbf{x}}_t; \alpha) = \frac{k_0}{2\pi} \int_{-\infty}^{\infty} \bar{\mathbf{E}}_0^w(\bar{\mathbf{x}}; \bar{\mathbf{x}}') e^{-ik_0 \alpha(z-z')} d(z-z') \quad (3)$$

where $\bar{\mathbf{E}}_0^w(\bar{\mathbf{x}}; \bar{\mathbf{x}}')$ is the field of a ring of axially-directed electric dipoles of radius a , located at a point $\bar{\mathbf{x}}'$ in the absence of the wire. $\bar{\mathbf{E}}_0^w(\bar{\mathbf{x}}_t; -\alpha)$ is thus the electric field produced by an axial current of the form $\exp(-ik_0 \alpha z')$ on the wire. $\bar{\mathbf{J}}_e^{\text{ext}}$, on the other hand, represents the external electric current source: the arbitrarily-oriented dipole in the present context which is given by

$$\bar{\mathbf{J}}_e^{\text{ext}}(\bar{\mathbf{x}}) = \bar{\mathbf{a}}_e p \delta(x-x_0) \delta(y-y_0) \delta(z-z_0) \quad (4)$$

In all the above, $\bar{\mathbf{x}}_t = (x, y)$ denotes the part of $\bar{\mathbf{x}}$ transverse to z .

From the geometry of Fig. 2, we have:

$$\bar{\mathbf{a}}_e = \bar{\mathbf{a}}_x \cos\theta + \bar{\mathbf{a}}_y \sin\theta \cos\phi + \bar{\mathbf{a}}_z \sin\theta \sin\phi \quad (5)$$

while $p = Id\ell$ is the dipole moment, and $\eta_0 = (\mu_0/\epsilon_0)^{1/2}$ is the wave impedance of free space.

The function $\tilde{M}(\alpha)$ is the characteristic modal expression for the wire [4]:

$$\tilde{M}(\alpha) = J_0(A\zeta) \left\{ \zeta^2 [H_0^{(1)}(A\zeta) - H_0^{(1)}(2H\zeta) J_0(A\zeta)] + J_0(A\zeta) [P(\alpha) - \alpha^2 Q(\alpha)] \right\} \quad (6)$$

where $A = k_0 a$ and $H = k_0 h$ are the normalized radius and height of the wire and J_0 and $H_0^{(1)}$ are the Bessel function and the Hankel function of

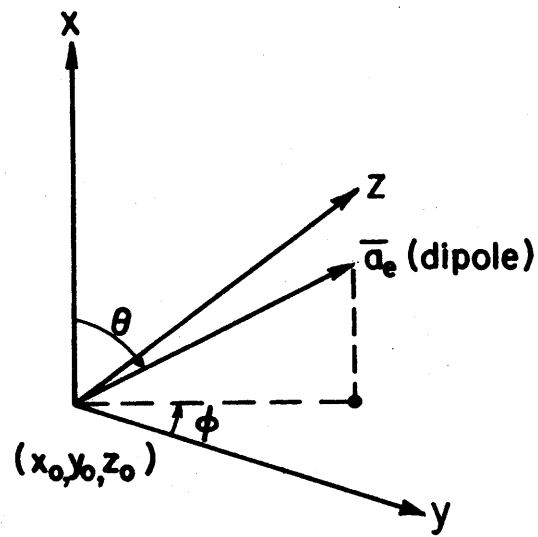


Figure 2. Dipole orientation

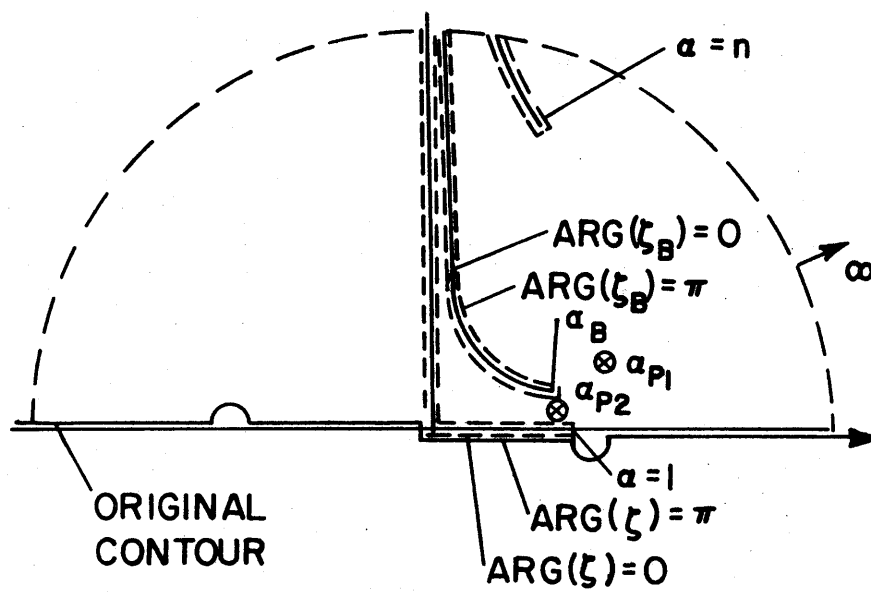


Figure 3. Deformation of contour in the complex α -plane

first kind respectively. P and Q are defined as Sommerfeld integrals:

$$P(\alpha) = P(H, 0; \alpha) \quad , \quad Q(\alpha) = Q(H, 0; \alpha)$$

where

$$P(X, Y; \alpha) = \frac{2}{i\pi} \int_{-\infty}^{\infty} \frac{\exp(-u_1 X + i\lambda Y)}{u_1 + u_2} d\lambda \quad (7)$$

$$Q(X, Y; \alpha) = \frac{2}{i\pi} \int_{-\infty}^{\infty} \frac{\exp(-u_1 X + i\lambda Y)}{n^2 u_1 + u_2} d\lambda \quad (8)$$

wherein

$$u_1 = (\lambda^2 - \zeta^2)^{\frac{1}{2}}, \quad u_2 = (\lambda^2 - \zeta_n^2)^{\frac{1}{2}}; \quad \text{Re}(u_1, u_2) \geq 0 \quad (9)$$

$$\zeta = (1 - \alpha^2)^{\frac{1}{2}}, \quad \zeta_n = (n^2 - \alpha^2)^{\frac{1}{2}}; \quad \text{Im}(\zeta, \zeta_n) \geq 0 \quad (10)$$

Approximate expressions for P and Q are given in Appendix A.

Inserting (4) and (5) into (2), we obtain

$$\gamma(\alpha) = \frac{4p}{\eta_0 k_0} \frac{\tilde{E}_e(\alpha)}{\tilde{M}(\alpha)} e^{-ik_0 \alpha z_0} \quad (11)$$

where

$$\tilde{E}_e(\alpha) = \bar{a}_e \cdot \tilde{E}_0^w(x_0, y_0; -\alpha) \quad (12)$$

$$= \tilde{E}_{ox}^w(x_0, y_0; -\alpha) \cos\theta + \tilde{E}_{oy}^w(x_0, y_0; -\alpha) \sin\theta \cos\phi + \tilde{E}_{oz}^w(x_0, y_0; -\alpha) \sin\theta \sin\phi$$

The components of \tilde{E}_0^w are given in Table 1 (see [4]). By superposition, we may now study a dipole of arbitrary orientation simply from a consideration of dipoles along the x, y , and z directions separately.

Finally, inserting (11) into (1), we have

Table 1

Components of $\tilde{E}_0^w(x_0, y_0; -\alpha)$	
$\tilde{E}_{0z}^w(x_0, y_0; -\alpha)$	$\frac{-k_0 \omega \mu_0}{8\pi} \left\{ \zeta^2 [H_0^{(1)}(\zeta R_{11}) - H_0^{(1)}(\zeta R_{12})] + P(X_0 + H, Y_0; \alpha) - \alpha^2 Q(X_0 + H, Y_0; \alpha) \right\}$ <p>P and Q are given by (7) and (8)</p>
$\tilde{E}_{0y}^w(X_0, Y_0; -\alpha)$	$\frac{i\omega \mu_0 k_0}{8\pi} \left\{ -\zeta \alpha \left[\frac{Y_0}{R_{11}} H_1^{(1)}(\zeta R_{11}) - \frac{Y_0}{R_{12}} H_1^{(1)}(\zeta R_{12}) \right] + \alpha \frac{\partial Q(X_0 + H, Y_0; \alpha)}{\partial Y_0} \right\}$
$\tilde{E}_{0x}^w(X_0, Y_0; -\alpha)$	$\frac{i\omega \mu_0 k_0}{8\pi} \left\{ \zeta \alpha \left[\frac{H - X_0}{R_{11}} H_1^{(1)}(\zeta R_{11}) - \frac{H + X_0}{R_{12}} H_1^{(1)}(\zeta R_{12}) \right] - n^2 \alpha \frac{\partial Q(X_0 + H, Y_0; \alpha)}{\partial X_0} \right\}$

$$X_0 = k_0 x_0, Y_0 = k_0 y_0, H = k_0 h, R_{11} = [Y_0^2 + (H - X_0)^2]^{\frac{1}{2}}, R_{12} = [Y_0^2 + (H + X_0)^2]^{\frac{1}{2}}$$

$$I(z) = \frac{4p}{\eta_0 k_0} \int_{-\infty}^{\infty} \frac{\tilde{E}_e(\alpha)}{\tilde{M}(\alpha)} e^{ik_0 \alpha (z-z_0)} d\alpha \quad (13)$$

Following [4,15], if $z-z_0 > 0$, we deform the contour of integration from the real axis of the α -plane upwards around three branch cuts emanating from $\alpha = 1$, $\alpha_B = n/(n^2+1)^{1/2}$, and n , respectively, as shown in Fig. 3. In this process, residues at the poles of the integrand (zeroes of $\tilde{M}(\alpha)$) are captured. Assuming the earth to be sufficiently lossy, the integral around the branch cut at $\alpha = n$ can be neglected [15], as can the residue at any pole which has a large imaginary part of α . In previous numerical studies [4, 13], two poles with small imaginary part have been found, so that under these conditions, the total current splits into four contributions:

$$I(z) = I_{p1}(z) + I_{p2}(z) + I_{B1}(z) + I_{B2}(z) \quad (14)$$

where I_{p1} and I_{p2} are residue terms from the poles at α_{p1} and α_{p2} , corresponding to discrete propagating modes, referred to as the structure-attached and surface-attached modes. We note that as earth becomes more conducting and/or operating frequency becomes lower the structure-attached mode is commonly known as the transmission-line mode because it approaches the ideal TEM-mode in the limit of $|n| \rightarrow \infty$, while I_{B1} and I_{B2} are the branch cut integrals around $\alpha = 1$ and $\alpha = \alpha_B$, respectively.

The two residue contributions have the form

$$I_p(z) = \frac{8p\pi i}{\eta_0 k_0} \frac{\tilde{E}_e(\alpha_p)}{\tilde{M}'(\alpha_p)} e^{ik_0 \alpha_p (z-z_0)} \quad (15)$$

The integral I_{B1} around the first branch cut, which corresponds to fields

radiated into the air--the "sky wave"--can be expressed as an integral along the real axis from 0 to 1, in addition to one along the positive imaginary axis:

$$I_{B1}(z) = \frac{4p}{\eta_0 k_0} \int_0^1 \frac{\tilde{M}_\pi(\alpha) \tilde{E}_{e0}(\alpha) - \tilde{M}_0(\alpha) \tilde{E}_{e\pi}(\alpha)}{\tilde{M}_0(\alpha) \tilde{M}_\pi(\alpha)} e^{ik_0 \alpha (z-z_0)} d\alpha - i \int_0^\infty \frac{\tilde{M}_\pi(i\alpha') \tilde{E}_{e0}(i\alpha') - \tilde{M}_0(i\alpha') \tilde{E}_{e\pi}(i\alpha')}{\tilde{M}_0(i\alpha') \tilde{M}_\pi(i\alpha')} e^{-k_0 \alpha' (z-z_0)} d\alpha' \quad (16)$$

where the subscripts "0" and " π " denote the argument of ζ .

The second branch cut integral, which corresponds to fields radiated at various directions along the ground, can be expressed as an integral with respect to a real variable by writing

$$\zeta_B = (\alpha_B^2 - \alpha^2)^{1/2} \quad (17)$$

where ζ_B is positive along the lower side of the branch cut. Changing the integration variable to ζ_B , we have

$$I_{B2}(z) = + \frac{4p}{\eta_0 k_0} \int_0^\infty \frac{\tilde{M}_\pi(\alpha) \tilde{E}_{e0}(\alpha) - \tilde{M}_0(\alpha) \tilde{E}_{e\pi}(\alpha)}{\tilde{M}_0(\alpha) \tilde{M}_\pi(\alpha)} e^{ik_0 \alpha (z-z_0)} \frac{\zeta_B d\zeta_B}{\alpha} \quad (18)$$

where $\alpha = (\alpha_B^2 - \zeta_B^2)^{1/2}$ and $\text{Im}(\alpha) > 0$. The subscripts 0 and π now refer to $\arg \zeta_B$ (i.e., the functions are evaluated at $+\zeta_B$ or $-\zeta_B$).

3. Current induced on the wire by a VED

In this section we present numerical results for the current induced by a vertical dipole in the xy-plane, at $x_0 = d$, $y_0 = b$. In this case,

the induced current is given by (13), with

$$\tilde{E}_e(\alpha) = \tilde{E}_{ox}^w(d, b; -\alpha) \quad (19)$$

and \tilde{E}_{ox}^w is given in Table 1. Accurate computational formulas for P , Q , and their derivatives needed in $\tilde{E}_e(\alpha)$ have been derived elsewhere [16] and are quoted in Appendix A.

In the first set of results presented here, the wire height in terms of the freespace wavelength λ is $h = 0.24\lambda$, the wire radius $a = 0.007\lambda$, and the refractive index of the earth is taken as $n = 5.3 + i0.45$. This situation corresponds to a rather poorly conducting earth, with $\epsilon/\epsilon_0 \approx 29$ and $\sigma \approx 27$ millimho/m at a frequency of 100MHz. The dipole strength was taken in all cases to be $Id\ell = .005$ amp-m. Fig. 4 shows the results of excitation by a VED located on the earth's surface below the wire ($d=0$, $b=0$) as a function of distance along the wire. Below about $z/\lambda = 0.1$, the integral (16) for I_{B1} , converges very slowly, and the numerical integration is quite time-consuming. It was, however, verified that the total current smoothly approaches zero as $z \rightarrow 0$, as required by expression (13), since \tilde{E}_{ox}^w is an odd function of α . We observe that the primary radiation current I_{B1} decays quickly with z , while I_{B2} drops off more slowly. Moreover, the pole term I_{p1} (which corresponds to a "structure-attached" or "transmission-line" mode) is initially the largest term, but decays more rapidly than I_{p2} (corresponding to the "surface-attached" or "earth-attached" mode). This latter mode, on the other hand, is excited much less efficiently than is the former, as might be expected since its fields are not as concentrated underneath the wire.

Fig. 5 shows the total current and its four components for a fixed

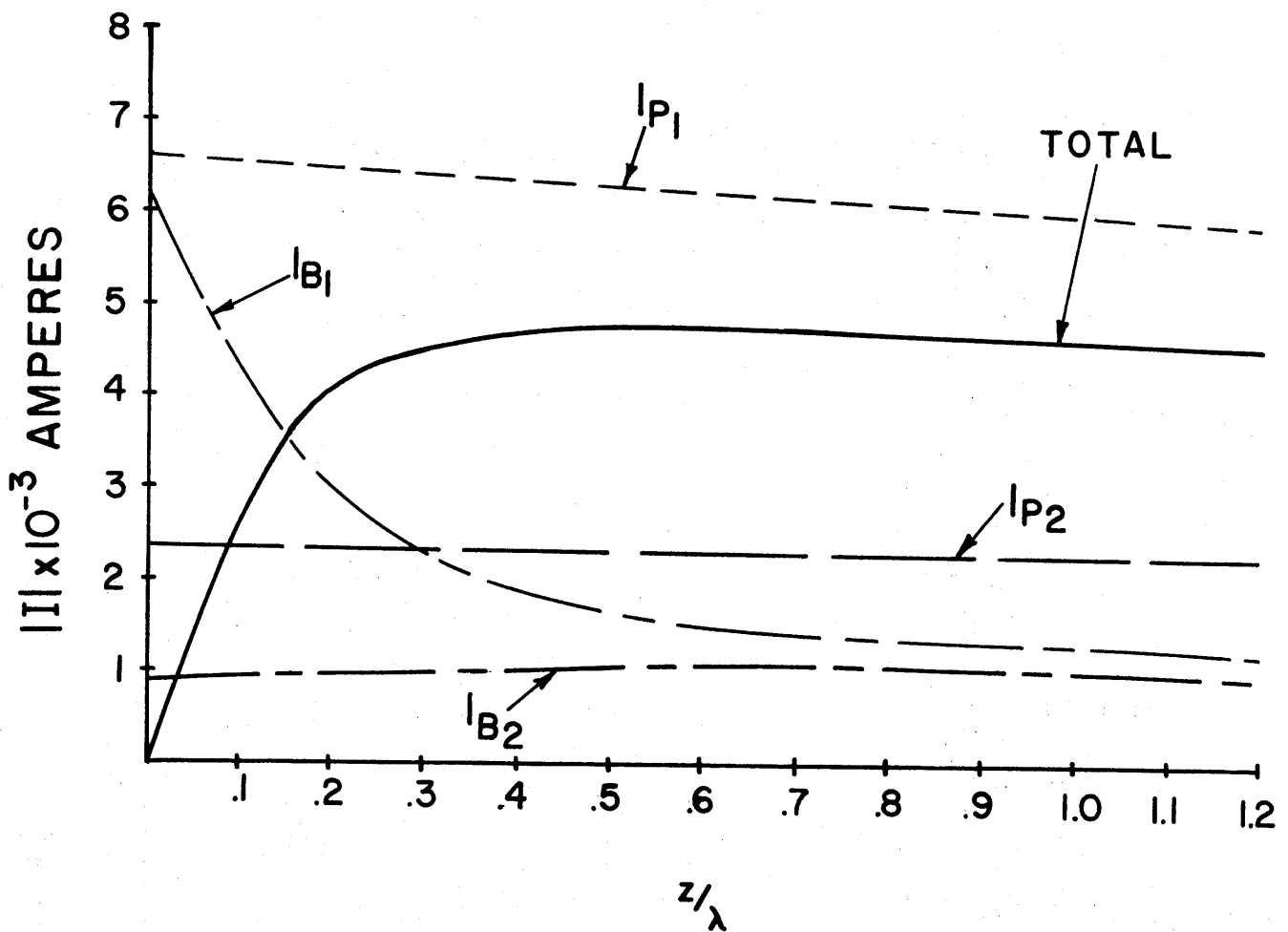


Figure 4: Current induced by a VED located under the wire at the earth's surface ($d = 0.0$, $b = 0.0$) vs. distance z along the wire; $n = 5.3 + i0.45$, $h = 0.24\lambda$, $a = .007\lambda$

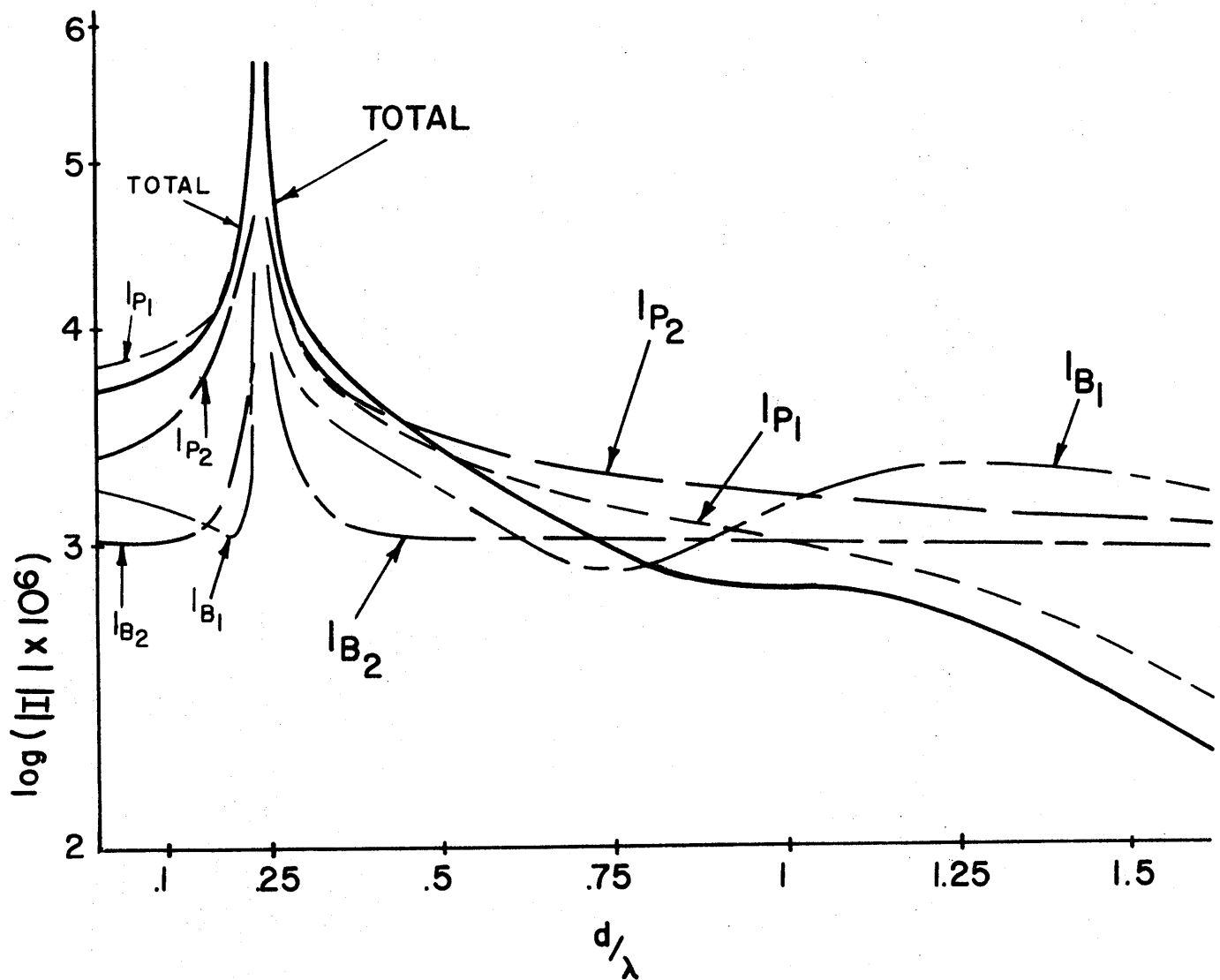


Figure 5. Current induced by a VED directly above and below the wire ($b=0.0$) as a function of height d for fixed distance $z=0.5\lambda$ along the wire; $n=5.3 + i0.45$, $h=0.24\lambda$, $a=.007\lambda$.

value of z as the height of the dipole is varied. At $d = h$, the dipole touches the wire and consequently the current becomes large in this vicinity. As d increases, the first branch cut current I_{B1} decays quickly after a few oscillations, while I_{B2} falls off more slowly. For sufficiently large heights, in fact, I_{B2} and I_{p2} , the current of the earth-attached mode, are the largest in magnitude, but substantially cancel each other as can be seen from the much smaller magnitude of the total current. For d smaller than h , it is clear that the major part of the current is that of the transmission-line mode, which is in agreement with the results of the previous figure. We note that the propagation constant α_{p1} of the transmission-line mode for this case is $0.99046 + i0.01562$, while that of the earth-attached mode α_{p2} is $0.99245 + i0.00239$. The branch point α_B is located at $0.98301 + i0.00283$.

In Fig. 6, a similar plot is shown for a somewhat larger value of $|n|$ and its loss tangent, $n = 7.43 + i6.73$. This case corresponds to a lower frequency (1MHz, say), $\epsilon/\epsilon_0 \approx 9.9$, and a rather smaller conductivity of $\sigma \approx 5.6$ millimho/m. In this case the transmission-line mode propagation constant $\alpha_{p1} = 1.0071 + i0.0113$, while that of the earth-attached mode $\alpha_{p2} = 0.9984 + i0.00371$. The branch point α_B is now situated at $0.99947 + i0.00494$. By comparison with Fig. 5, it can be seen that for this value of n the earth-attached mode is excited somewhat less efficiently when the dipole is located above the wire, indicating a greater spread of the fields of this mode in the region above the wire for the smaller value of n . This slower decay rate also appears in the slope of the second branch current I_{B2} and can be attributed to the decay rate of $\exp(-u_{1p}x)$ for the associated fields, where $u_{1p}^2 = -(n^2+1)^{-1}$. For Fig. 5 this value is

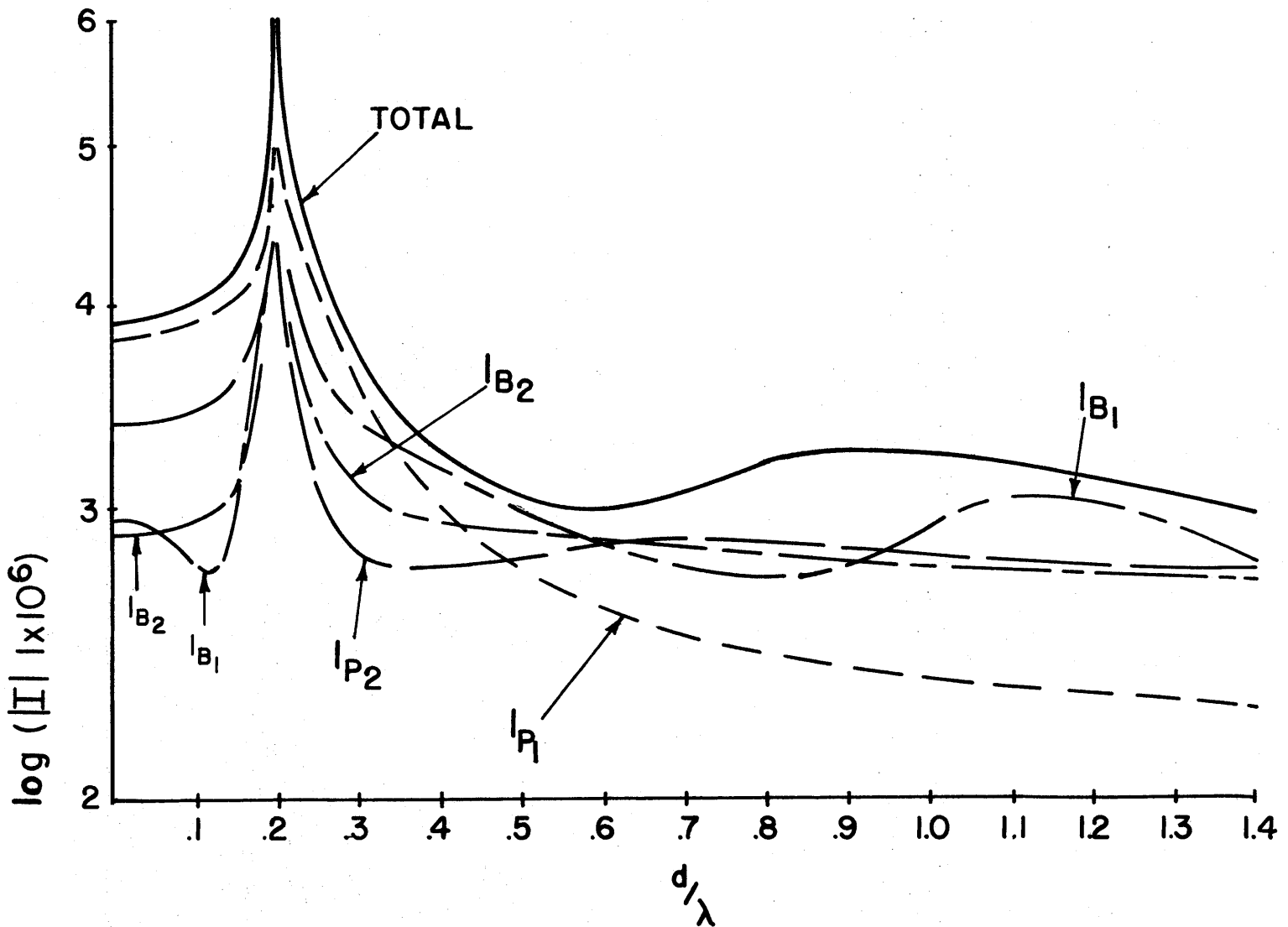


Figure 6. Current induced by a VED directly above and below the wire ($b = 0.0$) as a function of height d for fixed distance $z = 0.5\lambda$ along the wire; $n = 7.43 + i6.73$, $h = 0.2\lambda$, $a = .01\lambda$.

$u_{lp} = 0.00023 + i12.2$, while for Fig. 6, the decay rate is much faster since $u_{lp} = 0.0044 + i1.12$. In both cases, the wire has only a very localized effect on I_{B2} , while the parameters of the earth play a major role when the dipole is not close to the wire.

Figs. 7 and 8 examine the case when the dipole is located in the xy-plane at the earth's surface not directly under the wire ($x=0$, $y=b$). For a fixed observation point $z/\lambda = 0.5$, Fig. 7 shows the effect of varying b on the total current and its various components. For small b , the transmission-mode current dominates the total current, but falls off rapidly as b is increased. The earth-attached mode (I_{p2}) falls off more slowly, as expected, but by the time it reaches a magnitude comparable to that of I_{p1} , it is clear from the value of the total current that a good deal of mutual cancellation due to phase differences between the individual current contributions has taken place. In Fig. 8, the currents for a fixed value of $b(=1.0\lambda)$ are displayed as a function of distance along the wire. A broad maximum in the total current (due to a peak in I_{B1}) occurs in the neighborhood of $z = 0.12\lambda$, but otherwise there is little significant variation over a wavelength or two.

In Figs. 9-11, the current excited by a horizontal electric dipole (HED) is presented, all for the lower refractive index situation. Fig. 9 shows the results for an HED lying on the earth's surface at $b = 0.1\lambda$ as a function of distance along the wire. As was the case for Figs. 4 and 8 the transmission-line mode current I_{p1} is dominant except for z close to zero, when the first branch current I_{B1} becomes important (compare Fig. 4). It should be noted that the total current approaches zero as $z \rightarrow 0$ (as demanded by symmetry) and that a broad maximum occurs

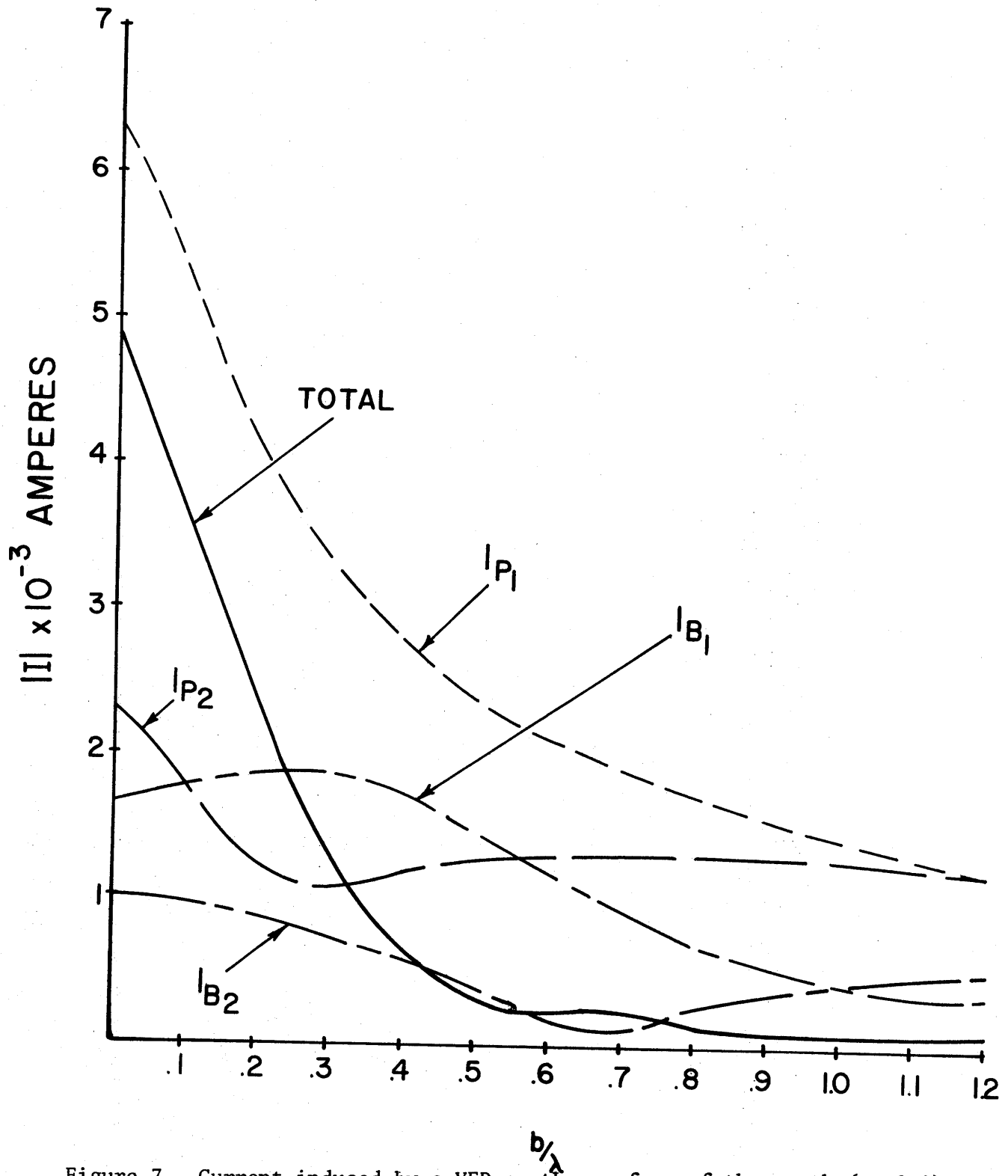


Figure 7. Current induced by a VED on the surface of the earth ($x=0.0$) as a function of the transverse displacement b for a fixed distance $z=0.5\lambda$ along the wire; $n = 5.3 + i0.45$, $h = 0.24\lambda$, $a = .007\lambda$.

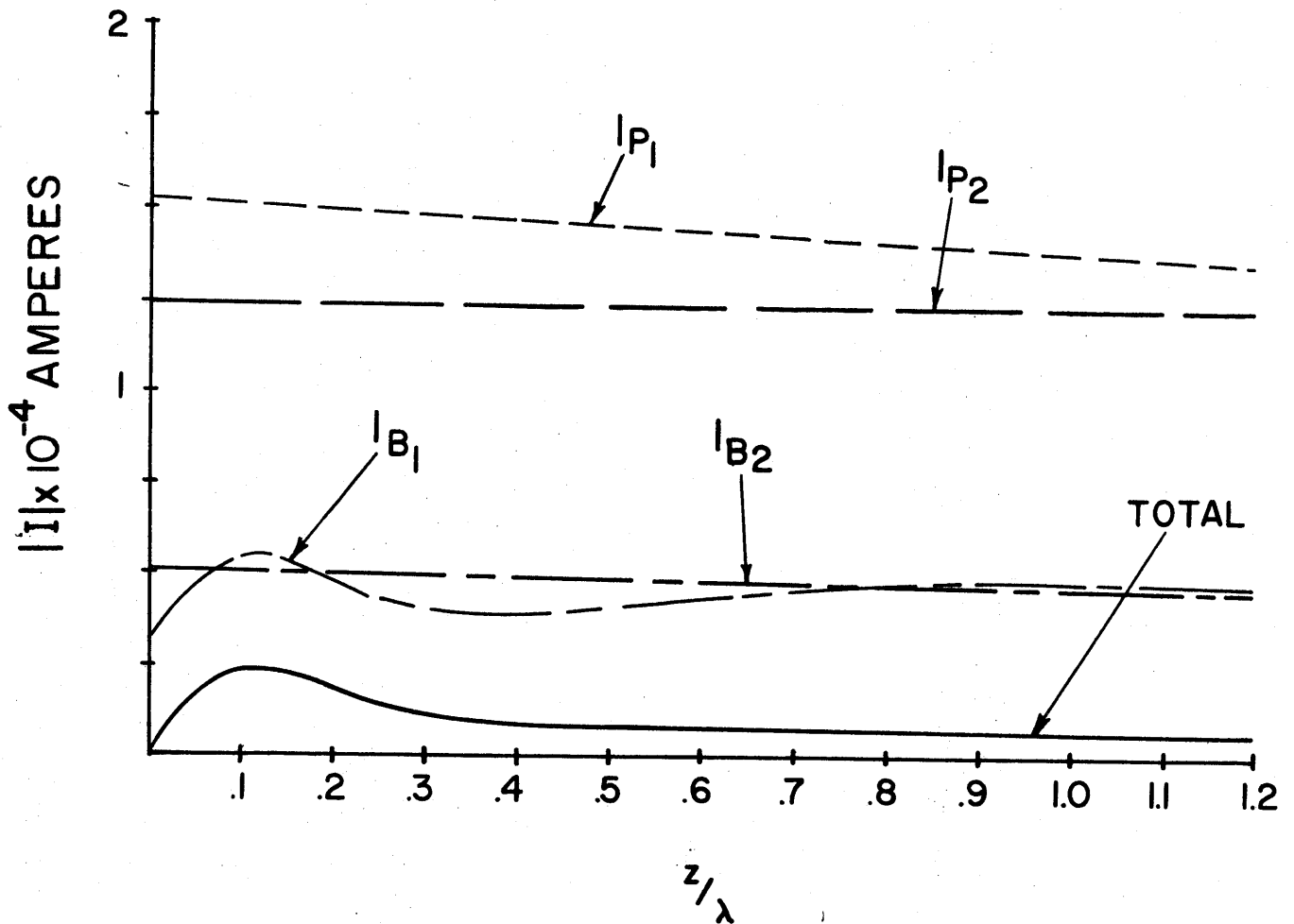


Figure 8. Current induced by a VED on the surface of the earth at $x/\lambda = 0.0$, $b/\lambda = 1.0$ as a function of distance z along the wire; $n = 5.3 + i0.45$, $h = 0.24\lambda$, $a = .007\lambda$.

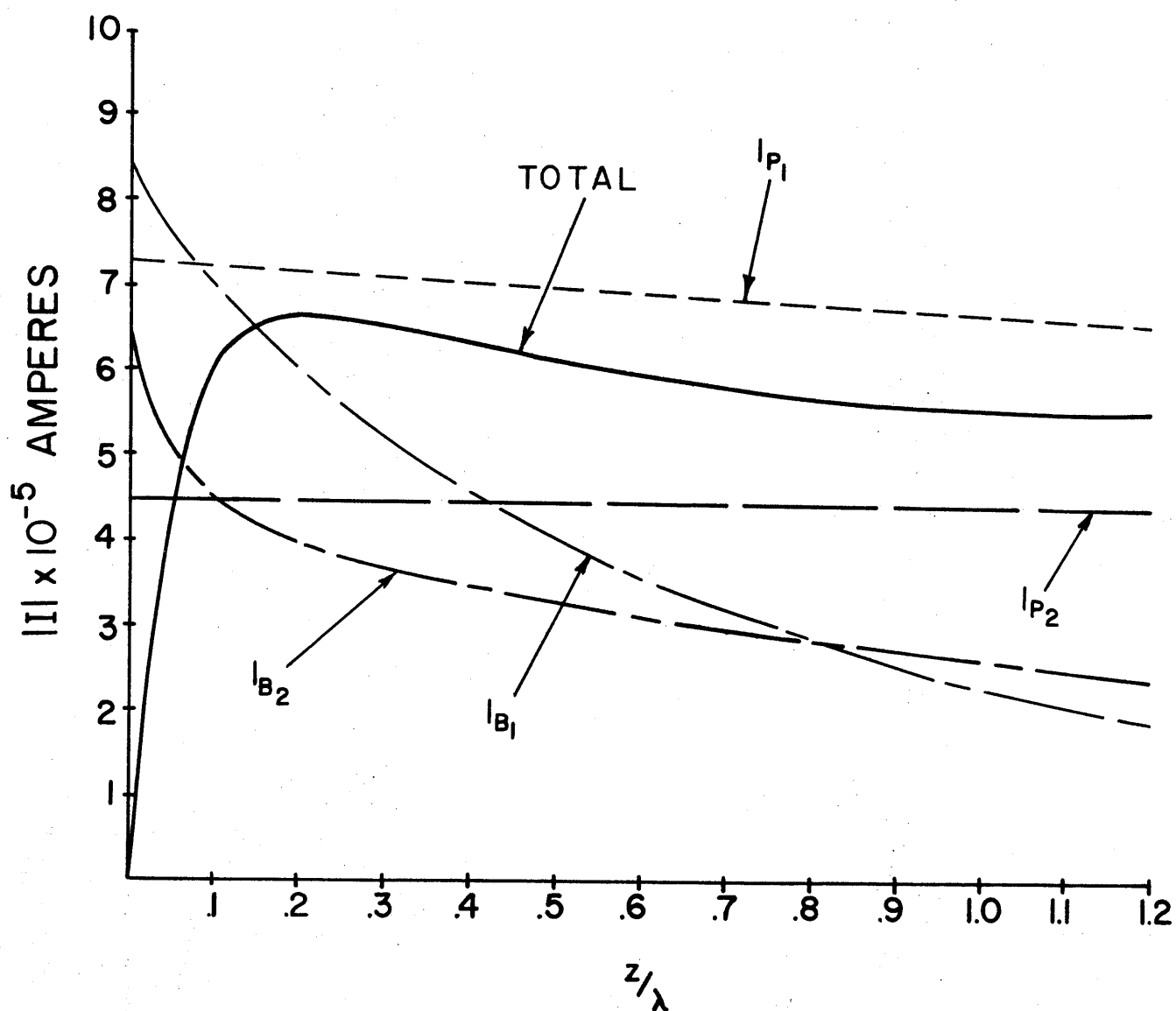


Figure 9. Current induced by an HED on the surface of the earth at $x/\lambda = 0.0$, $b/\lambda = 0.1$ as a function of the distance z along the wire; $n = 5.3 + i0.45$, $h = 0.24\lambda$, $a = .007\lambda$.

around $z = 0.2\lambda$. The second branch current I_{B2} is now much more significant compared to the earth-attached mode current I_{p2} than for the VED. Fig. 10 shows the currents for fixed z and b as a function of dipole height d . In contrast to Fig. 5, the transmission-mode current I_{p1} is the larger part of the total current, and little mutual cancellation between components of the current occurs, as indicated by the magnitude of the total current being always larger than those of its components. As expected, a maximum is found when the dipole height is equal to that of the wire. Fig. 11 displays the results for an HED located on the earth's surface as a function of the transverse displacement b . However, as in Fig. 7, substantial cancellation between individual current components is indicated for large values of b/λ . Note again that all currents vanish at $b = 0$, as demanded by symmetry. Overall, the total current induced on the wire is substantially smaller than that of a vertical dipole. This is particularly true when b/λ is smaller than 0.5 wavelength.

4. Scattering by an ellipsoidal dielectric obstacle

Of interest when using the wire over earth in a guided radar detection system is the effect on the wire currents of an obstacle in proximity to the wire. Human or animal intruders are modelled as lossy dielectric scatterers (because of the large water content [17]) while vehicles or other machinery must be represented as perfectly conducting bodies. If the dimensions of the scatterer are sufficiently small, and the incident field sufficiently uniform in the neighborhood of the scatterer, a Rayleigh or dipole approximation can be used to determine the scattered fields [14]. Even though the dimensions appropriate to a human intruder at the frequencies

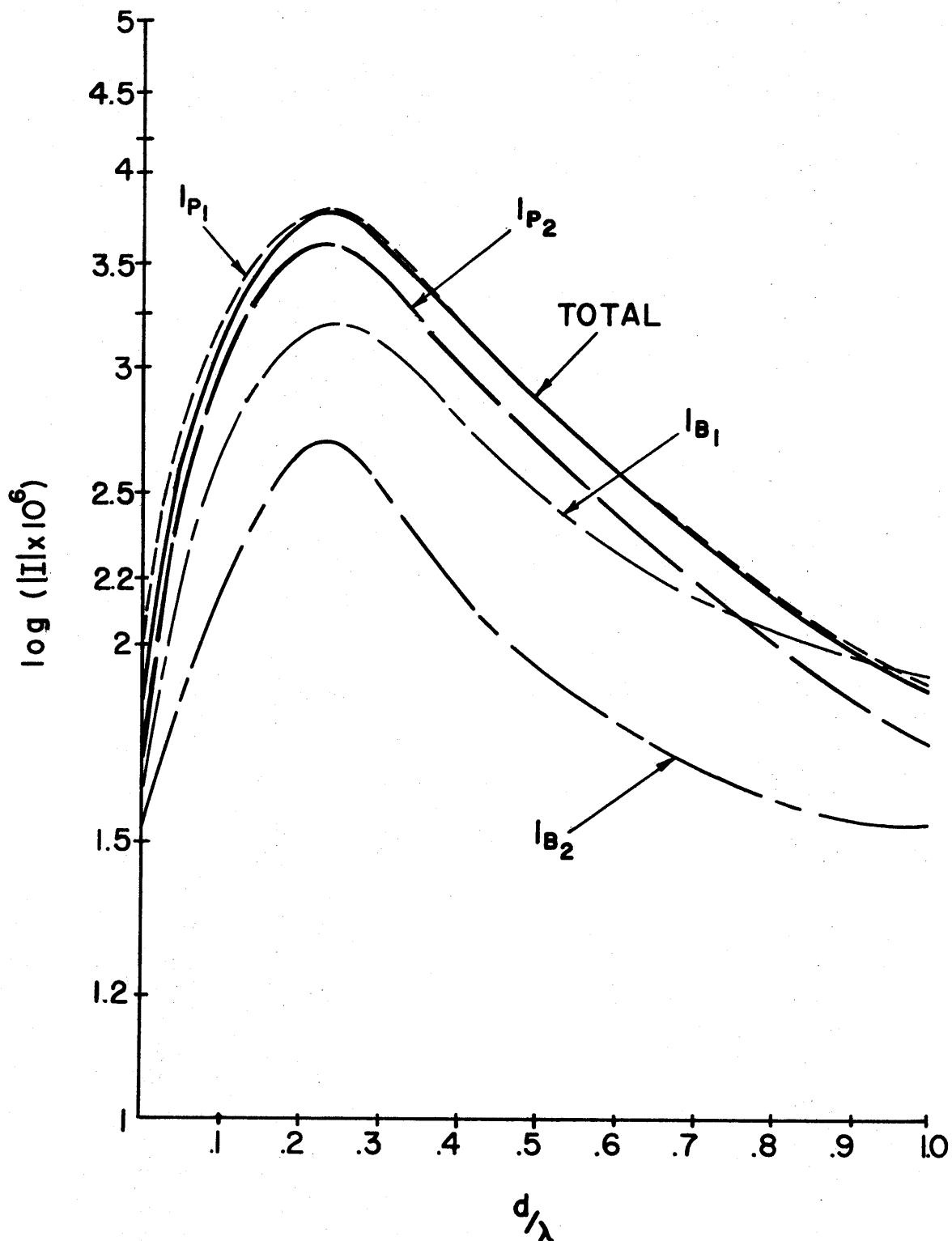


Figure 10. Current induced by an HED at $X = d$, $b/\lambda = 0.1$, $z/\lambda = 0.5$ as a function of height d ; $n = 5.3 + i0.45$, $h = 0.24\lambda$, $a = .007\lambda$.

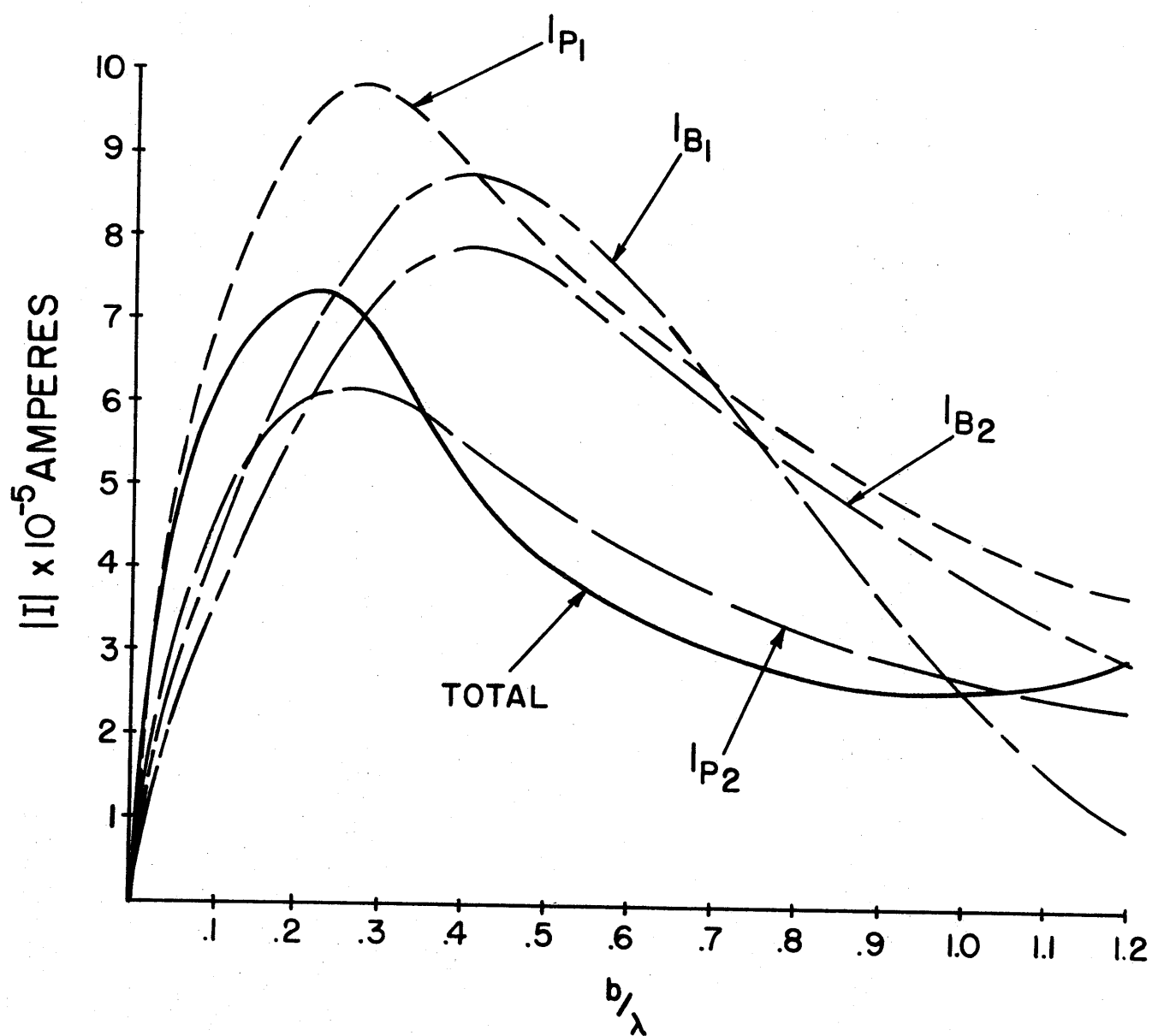


Figure 11. Current induced by an HED on the surface of the earth at $x/\lambda = 0.0$, $y = b$ at $z/\lambda = 0.5$, as a function of b ; $n = 5.3 + i0.45$, $h = 0.24\lambda$, $a = .007\lambda$.

considered in this report exceed those for which this approximation could be expected to be valid, it is reasonable to assume that such an approximation can still provide us with estimates of mode conversion due to the scatterer.

For simplicity we will restrict ourselves to consideration of an ellipsoidal dielectric obstacle with semi-axes as b , and c ($a > b = c$). A dielectric scatterer can be modelled by an electric dipole alone, while a metallic scatterer requires a magnetic dipole as well. If the ellipsoid is oriented along the vertical (x) axis, and an electric field E_{ox} is incident at the center of the obstacle, then the scattered field is approximately that produced by an x -directed electric dipole located at the center of the ellipsoid whose dipole moment is [14]

$$Idl = p = \frac{4}{3} \pi abc \omega P_x \quad (20)$$

where

$$P_x = \frac{\epsilon_0 E_{0x}}{I_1 + (N^2 - 1)^{-1}} \quad (21)$$

$$I_1 = \frac{b^2}{2a^2 e^3} \left[\ln \left(\frac{1+e}{1-e} \right) - 2e \right] \quad (22)$$

N is the refractive index of the ellipsoid, and e is its eccentricity given by

$$e^2 = 1 - \left(\frac{b}{a} \right)^2 \quad (23)$$

To model a human body, we used $N = 12.18 + i 8.27$, corresponding to $\epsilon_r = 80$ and $\sigma = 0.84$ mho/m at a frequency of 75 MHz, with $a/\lambda = 0.25$ and $b/\lambda = c/\lambda = 0.05$.

Using this approximation, the mode conversion caused by an obstacle whose center is located at $x/\lambda = 0.25$, $y = b$, $z = 0$ when the incident field is that of the structure-attached (transmission line) mode (α_{p1}) was computed and plotted out in Figs. 12 and 13. The incident current is taken to be unity at $z = 0$. Fig. 12 shows the percentage changes in the total current and its components relative to the amplitude of the unperturbed incident mode current in the absence of the scatterer at an observation point $z/\lambda = 2.0$, while Fig. 13 displays the same data for $z/\lambda = 20.0$. Although individual current components can be relatively quite large, it can be seen that a good deal of cancellation occurs among them. It should be noted that surface-attached mode I_{p2} at $z = 20.0\lambda$ has assumed a major importance because of the smaller attenuation of this mode than of I_{p1} . Additionally, the relative change in total current at $b = 0.2\lambda$ is 4% at 20 wavelengths, but only 1.3% at 2 wavelengths.

Figs. 14 and 15 give the corresponding results when the incident mode is the earth-attached mode (α_{p2}). At $z/\lambda = 2.0$ (Fig. 14), little difference from Fig. 12 is seen, except for minor qualitative changes attributable to the difference in field patterns of the incident modes. The relative change in total current at $b = 0.2\lambda$ is 1.0%. At $z = 20.0\lambda$ (Fig. 15), these qualitative differences are exaggerated, but it is important to note that because of the lower attenuation rate of the incident mode in this case, the relative change in total current at $b = 0.2\lambda$ is now smaller, about 0.7%.

We must emphasize again that the obstacle dimensions used here are larger than those for which the Rayleigh approximation could be considered valid; however, they are not inordinately large and should

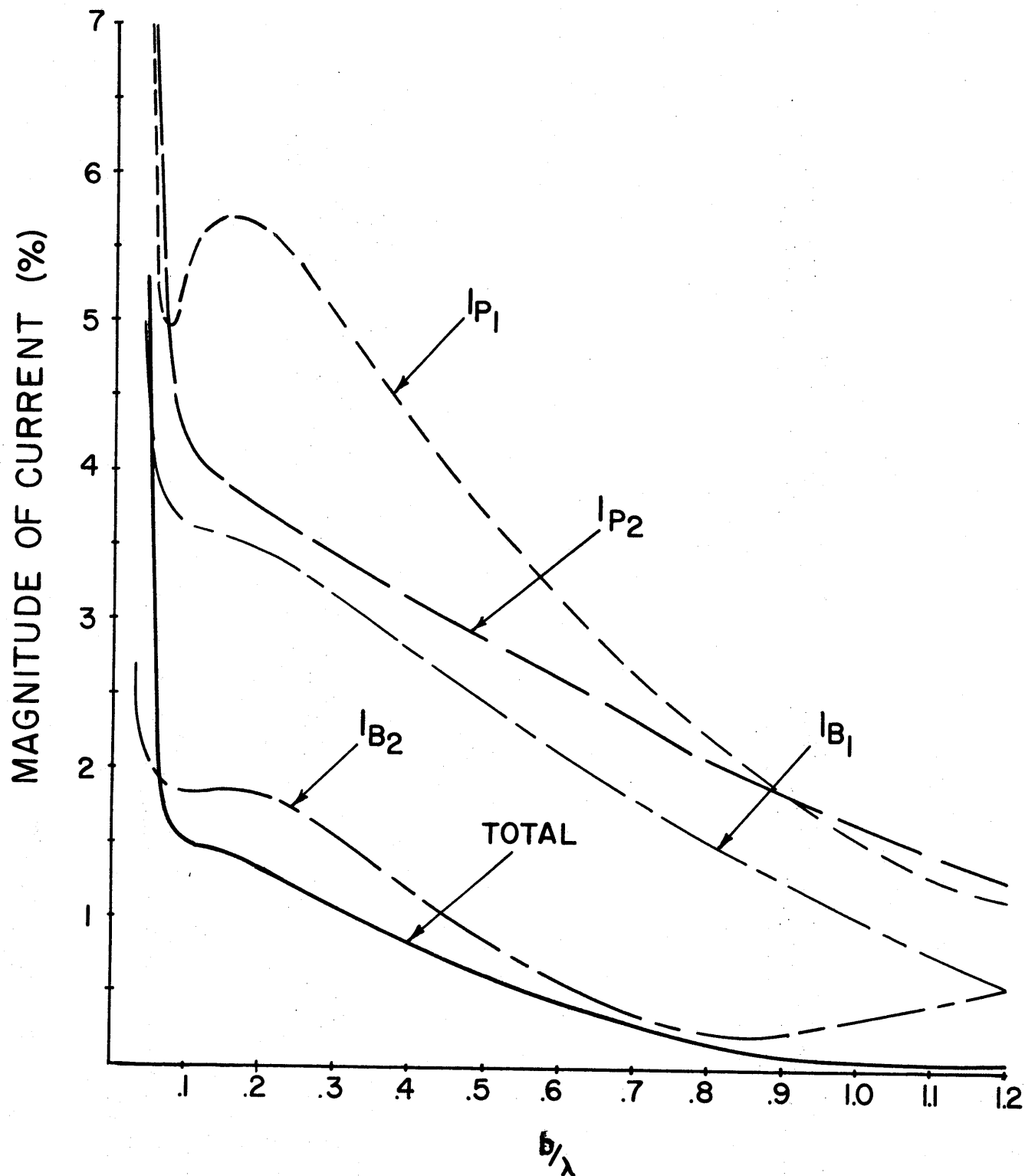


Figure 12. Change in current due to scattering of transmission line mode ($\alpha_{p1} = .99046 + i0.0156$) from ellipsoidal obstacle located at $y = b$; $n = 5.2 + i0.45$, $h = 0.24\lambda$, $a = .007\lambda$, $z = 2.0\lambda$.

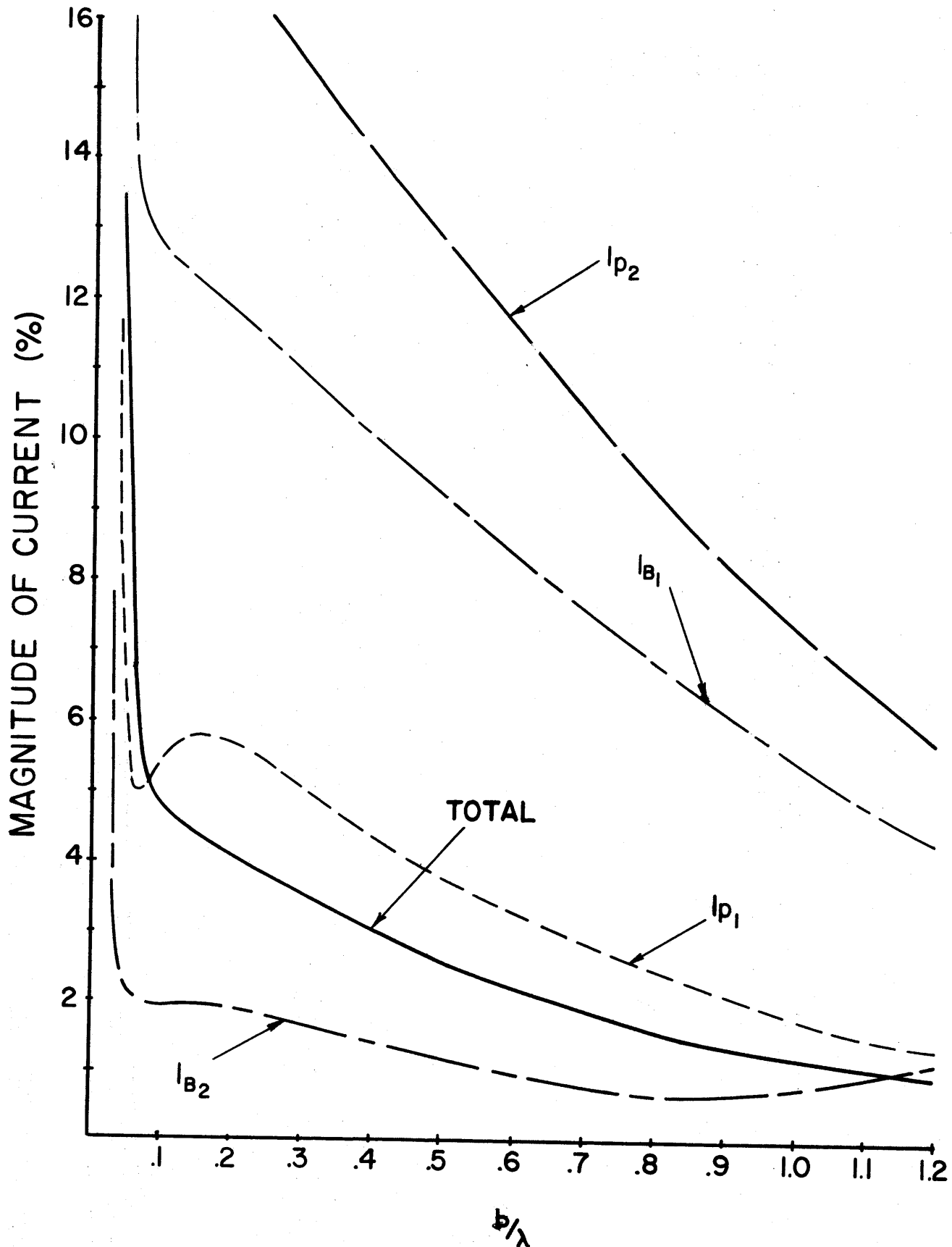


Figure 13. Change in current due to scattering of transmission line mode ($\alpha_{p1} = .99046 + i0.0156$) from ellipsoidal obstacle located at $y = b$; $n = 5.3 + i0.45$, $h = 0.24\lambda$, $a = .007\lambda$, $z = 20.0\lambda$.

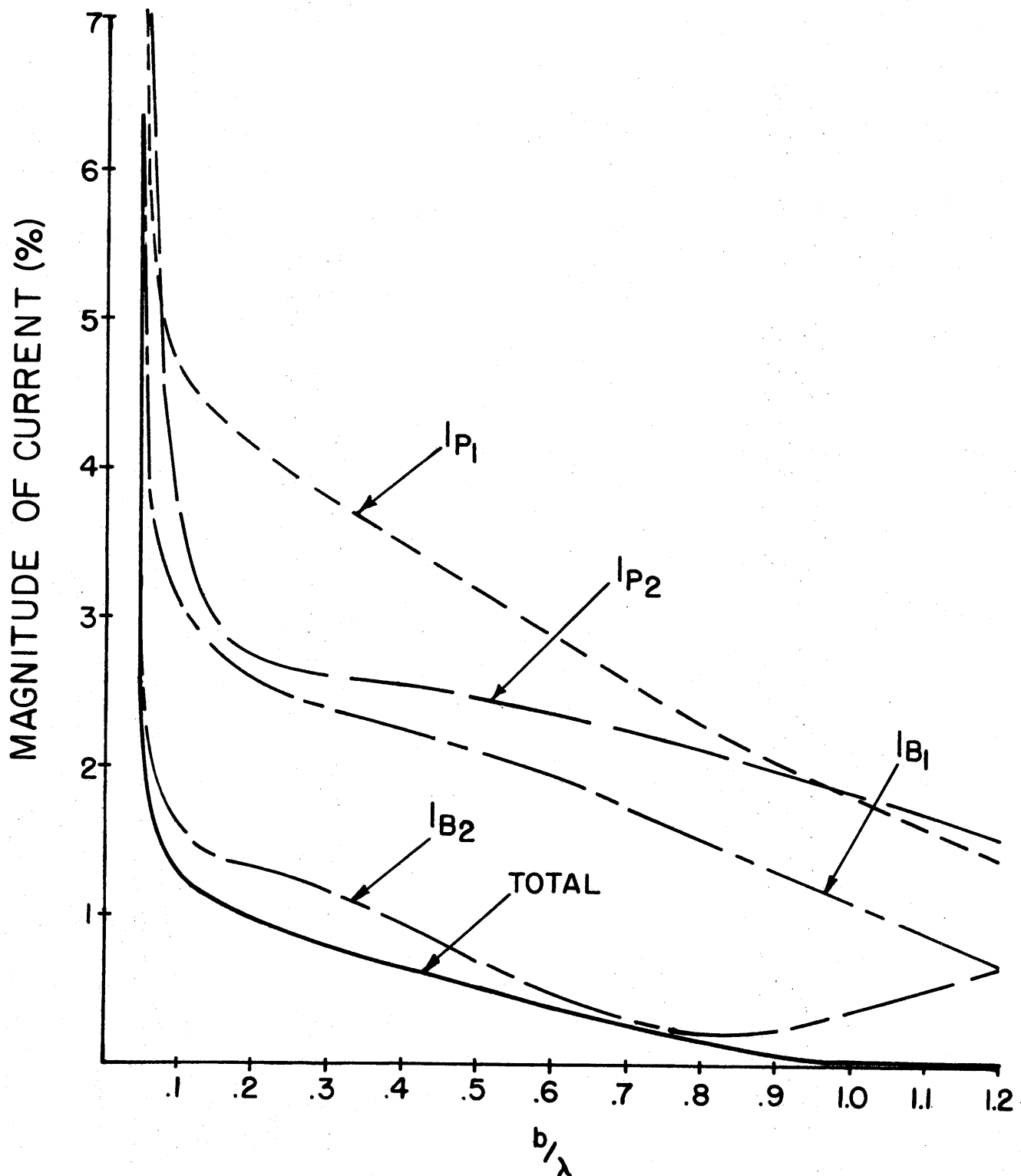


Figure 14. Change in current due to scattering of earth-attached mode ($\alpha_{p2} = .99245 + i0.00239$) from ellipsoidal obstacle located at $y = b$; $n = 5.3 + i0.45$, $h = 0.24\lambda$, $a = .007\lambda$, $z = 2.0\lambda$.

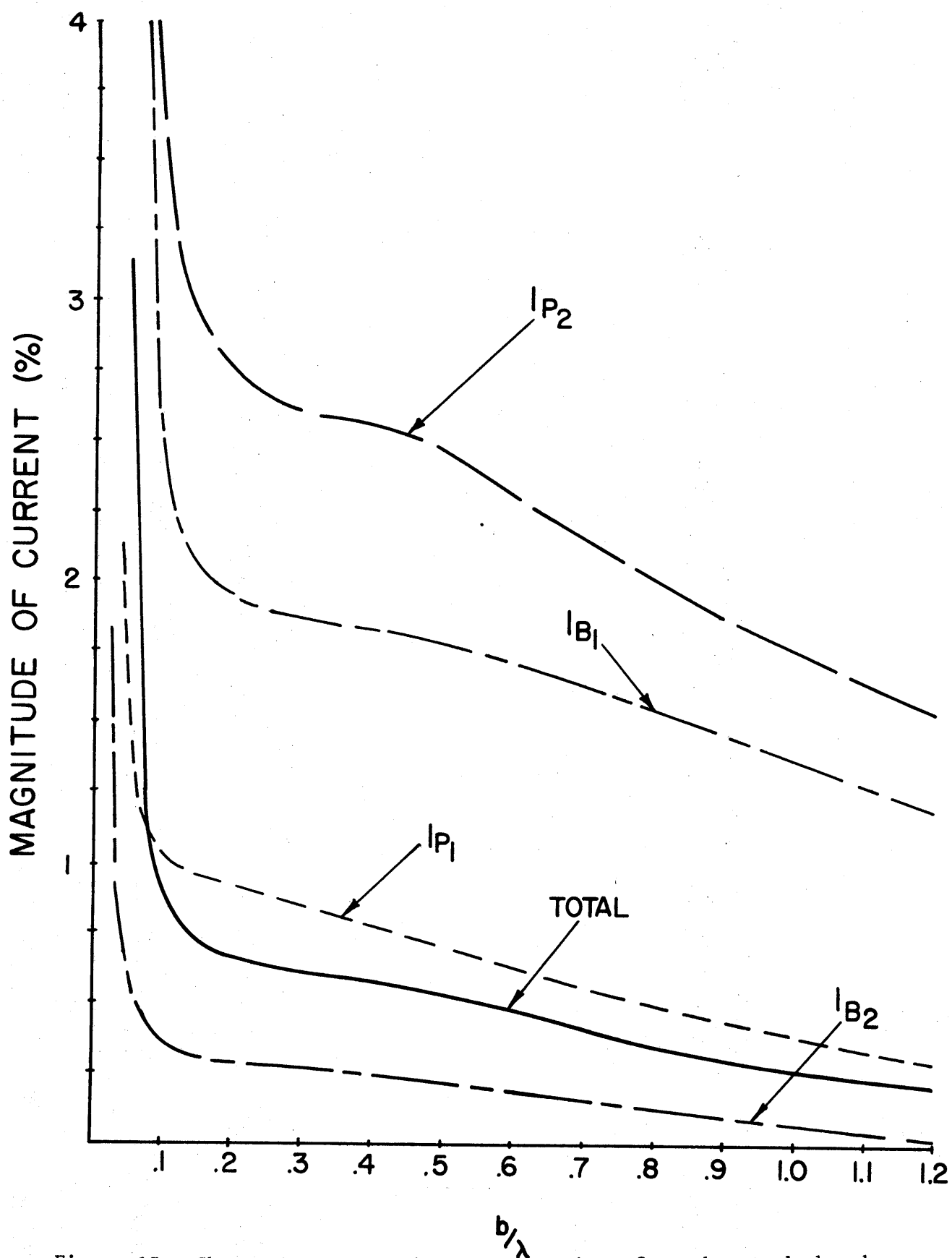


Figure 15. Change in current due to scattering of earth-attached mode ($\alpha_{p2} = .99245 + i0.00239$) from ellipsoidal obstacle located at $x = 0.5, y = 0.5, z = 0.5, h = 0.24, \epsilon = 0.07, \mu = 20.0$

provide reasonable estimates for the scattering from obstacles of similar size.

5. Conclusion

Although no dipole excitation considered here proved able to excite the earth-attached mode as the dominant part of the total current on the wire, this mode was in many cases comparable to the total current, and suitable tailoring of sources should be possible such that the amplitude of this mode is enhanced in relation to the others.

Somewhat paradoxically, it was found that an incident transmission-line mode provided a larger relative change in total current at large values of z , at least in part because it attenuates more rapidly than does the earth-attached mode. In actual practice, a localized generator (such as a delta-function voltage source) may be the excitation scheme used, and both discrete modes as well as radiation modes may well be incident on the obstacle. Although the analysis of this problem requires the computation of radiation fields and not just currents (this will be taken up in a future report), some predictions on the basis of previous work can be made. In [15] it is shown that the transmission-line mode is excited most efficiently by a delta-function generator when the wire height is less than about 0.15λ above the earth. This seems to indicate that, contrary to the intuition which states that a large wire height will produce more field spread and better detection, in fact a relatively small wire height might be most efficient, in so far as providing a larger percentage of changes along the wire at least for a bare wire.

It is clear from Figs. 12-15 that if information about individual

current components could be obtained, then considerably more sensitive detection could take place. At present, however, the authors are unaware of such a selective detection scheme, and suggest that a search for one would be worthwhile.

Appendix A

Approximate formulas for the integrals in Table 1.

The integrals appearing in Table 1 are P, Q, and the derivatives of Q with respect to x and with respect to y, where the integrals P and Q are given by (7) and (8). It is thus sufficient to obtain computational expressions for P and Q alone, and the remaining integrals can be obtained by formal differentiation. The desired expressions for P and Q have been derived in [16]. Only the approximate forms valid for $2|n^2|k_0^2(x+d)^2 \gg 1$ and $|n|^2 \gg 1$ (which are essentially obtained by setting $u_2 = -in$ in (7) and (8) [13,16]) will be quoted here:

$$P(X,Y;\alpha) \approx \frac{2}{(n^2-1)} \{ \zeta H_1^{(1)}(\zeta R_{12}) \left[\frac{i\zeta_n X}{R_{12}} + \frac{X^2 - Y^2}{R_{12}^3} \right] - \frac{\zeta^2 X^2}{R_{12}^2} H_0^{(1)}(\zeta R_{12}) \} \quad (A.1)$$

where $R_{12} = [Y^2 + (X+H)^2]^{\frac{1}{2}}$. In addition

$$Q(X,Y;\alpha) \approx \frac{2}{n} H_0^{(1)}(\zeta R_{12}) + \frac{2}{\pi n} W(X,Y;\alpha) \quad (A.2)$$

where

$$W(X,Y;\alpha) = [W_X(X,Y;\alpha) + W_0(Y;\alpha)] \exp[-i(X+H)/n] \quad (A.3)$$

The function W_0 is given by

$$W_0(Y;\alpha) = \frac{\pi i}{\zeta_B} \exp(i\zeta_B Y) + \frac{\pi}{n\zeta_B} S(Y) + \cos(\zeta_B Y) W_{02}(\alpha)$$

$$W_{02}(\alpha) = \mp \frac{i\pi}{\zeta_B} + \frac{2i}{(1/n^2 - \zeta^2)^{\frac{1}{2}}} \{ \ln \left[\frac{1}{n} + \left(\frac{1}{n^2} - \zeta^2 \right)^{\frac{1}{2}} \right] - \ln |\zeta| \} \quad (A.4)$$

with $\zeta_B = (\alpha_B^2 - \alpha^2)^{\frac{1}{2}}$; $\text{Im}(\alpha_B) \geq 0$, while the explicit square roots in $W_{02}(\alpha)$ are to have positive real part and the principal branch of the logarithm is to be taken. The minus or plus sign is to be taken according to whether $\arg(\zeta) = 0$ or π respectively, on the first branch cut; the minus sign is to be taken on both sides of the second branch cut, and at all other points in the first quadrant of the α -plane. S is expressible as an infinite series whose coefficients are defined recursively:

$$S(Y) = \frac{iY}{2} \sum_{m=0}^{\infty} \frac{(i\zeta_B Y)^m}{m!} [e^{-i\zeta_B Y} - (-1)^m e^{i\zeta_B Y}] I_m(\zeta Y) \quad (\text{A.5})$$

$$I_0(\zeta Y) = H_0^{(1)}(\zeta Y) + \frac{\pi}{2} [H_0(\zeta Y) H_1^{(1)}(\zeta Y) - H_1(\zeta Y) H_0^{(1)}(\zeta Y)]$$

$$I_1(\zeta Y) = (\zeta Y)^{-1} [H_1^{(1)}(\zeta Y) + \frac{2i}{\pi \zeta Y}]$$

$$I_m(\zeta Y) = (\zeta Y)^{-1} H_1^{(1)}(\zeta Y) + (m-1)(\zeta Y)^{-2} H_0^{(1)}(\zeta Y) - (m-1)^2 (\zeta Y)^{-2} I_{m-2}(\zeta Y); \quad m \geq 2$$

where $H_j(X)$ is the Struve function of order j .

In similar fashion, the function W_X is given by

$$W_X(X, Y; \alpha) = -i\pi \sum_{m=0}^{\infty} \frac{f^{[m]} \left[\frac{(X+H)^2}{2} + Y^2 \right]}{m!} (X+H)^{2m+1} L_m \left(\frac{i[X+H]}{n} \right) \quad (\text{A.6})$$

where again, the coefficients are defined recursively:

$$\left. \begin{aligned} f^{(0)}(\theta) &= H_0^{(1)}(\zeta \theta^{\frac{1}{2}}) \\ f^{(1)}(\theta) &= -\frac{\zeta}{2\theta^{\frac{1}{2}}} H_1^{(1)}(\zeta \theta^{\frac{1}{2}}) \\ f^{[m]}(\theta) &= -\theta^{-1} [(m-1)f^{[m-1]}(\theta) + \frac{\zeta^2}{4} f^{[m-2]}(\theta)]; \quad m \geq 2 \end{aligned} \right\} \quad (\text{A.7})$$

$$\left. \begin{aligned}
 L_0(t) &= (e^t - 1)/t \\
 L_1(t) &= \{e^t - \frac{2}{t} [e^t - L_0(t)]\}/t - L_0(t)/2 \\
 L_m(t) &= t^{-1} \cdot \{2^{-m} [e^t - (-1)^m] - (\frac{2m}{t}) [2^{1-m} e^t] - \\
 &\quad - (2m-1)L_{m-1}(t) - (m-1)L_{m-2}(t)\} ; \quad m \geq 2
 \end{aligned} \right\} \quad (A.8)$$

Since expression (A.6) does not converge rapidly if Y is small compared to $X + H$, an alternative expression for W , useful when $(X + H)^2 \geq 2Y^2$, is needed:

$$W(X, Y; \alpha) = \cos(\zeta_B Y) W(X, 0; \alpha) - i\pi \sum_{m=1}^{\infty} \frac{(-1)^m Y^{2m}}{(2m)!} R_m(X; \alpha) \quad (A.9)$$

where

$$W(X, 0; \alpha) = \exp[-i(X + H)/n] \{-i\pi T(X) + W_{02}(\alpha) + \frac{i\pi}{\zeta_B}\} \quad (A.10)$$

$$T(X) = \sum_{m=0}^{\infty} \frac{\left[\frac{i(X+H)}{n} \right]^m}{m!} (X + H) I_m[\zeta(X+H)] \quad (A.11)$$

with I_m given by (A.5) and $W_{02}(\alpha)$ by (A.4). The functions R_m are defined recursively

$$\begin{aligned}
 R_0(X; \alpha) &= 0 \\
 R_m(X; \alpha) &= (\zeta^2 + \zeta_B^2) R_{m-1}(X; \alpha) + g_{m-1}(X; \alpha); \quad m \geq 1 \\
 g_m(X; \alpha) &= \frac{\partial^{2m}}{\partial X^{2m}} \left[\frac{\partial}{\partial X} - \frac{i}{n} \right] H_0^{(1)}(\zeta X)
 \end{aligned} \quad (A.12)$$

Comparison between the formulas in this section and the exact values of P and Q has demonstrated their accuracy for practical computations [16].

As seen in Table 1, it may be necessary to evaluate $\frac{\partial Q}{\partial X}$ or $\frac{\partial Q}{\partial Y}$ for certain dipole orientations. Computational formulas for these quantities can be obtained by formal differentiation of the expressions given in this Appendix.

References

- [1] J.R. Carson, "Wave propagation in overhead wires with ground return," Bell Syst. Tech. J. v.5, pp. 539-554 (1926).
- [2] G.A. Grinberg and B. E. Bonshtedt, "Foundations of an exact theory of transmission line fields," Zh Tekh. Fiz. v. 24, pp. 67-95 (1954) [in Russian].
- [3] J.R. Wait, "Theory of wave propagation along a thin wire parallel to an interface," Radio Science v. 7, pp. 675-679 (1972).
- [4] E.F. Kuester and D. C. Chang, "Modal representation of a horizontal wire above a finitely conducting earth," Sci.Rept. No. 21 (RADC-TR-76-287), Dept. Elec. Eng., Univ. of Colorado, Boulder (1976).
- [5] J.R. Wait, "Excitation of a coaxial cable or wire conductor located over the ground by a dipole radiator," Arch. Elek, Übertrag. v. 31, pp. 121-127 (1977).
- [6] R.G. Olsen and M.A. Usta, "The excitation of current on an infinite horizonatl wire above earth by a vertical electric dipole," IEEE Trans. Ant. Prop. v. 25, pp. 560-565 (1977).
- [7] D.A. Hill and J.R. Wait, "Coupling between a dipole antenna and an infinite cable over an ideal ground plane," Radio Science v. 12, pp. 231-238 (1977).
- [8] F.H. Northover, "Radiation and surface currents from a slot on an infinite conducting cylinder," Canad. J. Phys. v. 36, pp. 206-217 (1958).
- [9] L. Shafai, "Excitation of a conducting cylinder by an axial electric dipole," Canad. J. Phys. v. 46, pp. 211-219 (1968).
- [10] R. Gerharz, "Wire-guided transients as remote sensing agents for material objects," Int. J. Electron. v. 42, pp. 439-445 (1977).
- [11] N.A. Mackay and D. G. Beattie, "High-resolution guided radar system," Electron. Lett. v. 12, pp. 583-584 (1976).
- [12] R.E. Patterson and N.A. Mackay, "A guided radar system for obstacle detection," IEEE Trans. Inst. Meas. v. 26, pp. 137-143 (1977).
- [13] R.G. Olsen and D.C. Chang, "Electromagnetic characteristics of a horizontal wire above a dissipative earth--Part I: Propagation of transmission-line and fast-wave modes," Sci. Rept. No. 3 (NOAA-N22-126-72) Dept. of Elec. Eng., Univ. of Colorado, Boulder (1953).
- [14] D.S. Jones, The Theory of Electromagnetism. Oxford: Pergamon Press, 1964, pp. 528-532.
- [15] D.C. Chang and R.G. Olsen, "Excitation of an infinite antenna above a dissipative earth," Radio Science v. 10, pp. 823-831 (1975).

- [16] S.W. Plate, D.C. Chang and E.F. Kuester, "Characteristic of discrete propagation modes on a system of horizontal wires over a dissipative earth," Sci. Rept. No. 24 (RADC-TR-77-81) Dept. of Elec. Eng., Univ. of Colorado, Boulder (1977).
- [17] K.-M. Chen and B.S. Guru, "Internal EM field and absorbed power density in human torsos induced by 1-500 MHz EM waves," IEEE Trans. Micr. Theory Tech.v. 25, pp. 746-756 (1977)

List of Figures

- Fig. 1: Geometry of the problem
- Fig. 2: Dipole orientation
- Fig. 3: Deformation of contour in the complex α -plane
- Fig. 4: Current induced by a VED located under the wire at the earth's surface ($d = 0.0$, $b = 0.0$) vs. distance z along the wire; $n = 5.3 + i0.45$, $h = 0.24\lambda$, $a = .007\lambda$.
- Fig. 5: Current induced by a VED directly above and below the wire ($b = 0.0$) as a function of height d for fixed distance $z = 0.5\lambda$ along the wire; $n = 5.3 + i0.45$, $h = 0.24\lambda$, $a = .007\lambda$.
- Fig. 6: Current induced by a VED directly above and below the wire ($b = 0.0$) as a function of height d for fixed distance $z = 0.5\lambda$ along the wire; $n = 7.43 + i6.73$, $h = 0.2\lambda$, $a = .01\lambda$.
- Fig. 7: Current induced by a VED on the surface of the earth ($x = 0.0$) as a function of the transverse displacement b for a fixed distance $z = 0.5\lambda$ along the wire; $n = 5.3 + i0.45$, $h = 0.24\lambda$, $a = .007\lambda$.
- Fig. 8: Current induced by a VED on the surface of the earth at $x/\lambda = 0.0$, $b/\lambda = 1.0$ as a function of distance z along the wire; $n = 5.3 + i0.45$, $h = 0.24\lambda$, $a = .007\lambda$.
- Fig. 9: Current induced by an HED on the surface of the earth at $x/\lambda = 0.0$, $b/\lambda = 0.1$ as a function of the distance z along the wire; $n = 5.3 + i0.45$, $h = 0.24\lambda$, $a = .007\lambda$.
- Fig. 10: Current induced by an HED at $x = d$, $b/\lambda = 0.1$, $z/\lambda = 0.5$ as a function of height d ; $n = 5.3 + i0.45$, $h = 0.24\lambda$, $a = .007\lambda$.
- Fig. 11: Current induced by an HED on the surface of the earth at $x/\lambda = 0.0$, $y = b$ at $z/\lambda = 0.5$, as a function of b ; $n = 5.3 + i0.45$, $h = 0.24\lambda$, $a = .007\lambda$.
- Fig. 12: Change in current due to scattering of transmission line mode ($\alpha_{p1} = .99046 + i0.0156$) from ellipsoidal obstacle located at $y = b$; $n = 5.2 + i0.45$, $h = 0.24\lambda$, $a = .007\lambda$, $z = 2.0\lambda$.
- Fig. 13: Change in current due to scattering of transmission line mode ($\alpha_{p1} = .99046 + i0.0156$) from ellipsoidal obstacle located at $y = b$; $n = 5.3 + i0.45$, $h = 0.24\lambda$, $a = .007\lambda$, $z = 20.0\lambda$.
- Fig. 14: Change in current due to scattering of earth-attached mode ($\alpha_{p2} = .99245 + i0.00239$) from ellipsoidal obstacle located at $y = b$; $n = 5.3 + i0.45$, $h = 0.24\lambda$, $a = .007\lambda$, $z = 2.0\lambda$.
- Fig. 15: Change in current due to scattering of earth-attached mode ($\alpha_{p2} = .99245 + i0.00239$) from ellipsoidal obstacle located at $y = b$; $n = 5.3 + i0.45$, $h = 0.24\lambda$, $a = .007\lambda$, $z = 20.0\lambda$.